Two grapevine *metacaspase* genes mediate ETI-like cell death in grapevine defence against infection of *Plasmopara viticola*

Peijie Gong [1] · Michael Riemann [1] · Duan Dong [1] · Nadja Stoeffler [1] · Bernadette Gross [1] · Armin Markel [1] · Peter Nick [1]

Abstract

Metacaspase, as hypersensitive response (HR) executors, has been identified in many plant species. Previously, the entire gene family of metacaspase has been uncovered, but there are still questions that remain unclear regarding HR-regulating gene members. In this study, based on *metacaspase* expression during different grapevine genotypes interacting with *Plasmopara viticola*, we identified *MC2* and *MC5* as candidates involved in HR. We overexpressed both metacaspases as GFP fusions in tobacco BY-2 cells to address subcellular localization and cellular functions. We found MC2 located at the ER, while MC5 was nucleocytoplasmic. In these overexpressor lines, cell death elicited by the bacterial protein harpin, is significantly enhanced, indicating MC2 and MC5 mediated defence-related programmed cell death (PCD). This effect was mitigated, when the membrane-located NADPH oxidase was inhibited by the specific inhibitor diphenylene iodonium, or when cells were complemented with methyl jasmonate, a crucial signal of basal immunity. Both findings are consistent with a role of MC2 and MC5 in cell death-related immunity. Using a dual-luciferase reporter system in grapevine cells we demonstrated both *MC2* and *MC5* promoter alleles from *V. rupestris* were more responsive to harpin than those from *V. vinifera* cv 'Müller-Thurgau', while they were not induced by MeJA as signal linked with basal immunity. These findings support a model, where MC2 and MC5 act specifically as executors of the HR.

Keywords Metacaspase · Programmed cell death (PCD) · Plant immunity · *Vitis rupestris* · Hypersensitive response (HR)

Introduction

To cope with pathogens, plants have evolved a defence system consisting of multiple layers of innate immunity (Jones and Dangl 2006). Binding of general pathogen-associated molecular patterns (PAMPs) to receptors localised at the cell membrane can initiate a broad defence response against an entire group of pathogens, so-called PAMP triggered immunity (PTI). However, in consequence of an evolutionary arm race, adapted microbial pathogens have developed secreted molecules, so-called effectors, that are able to suppress PTI and to reinstall infection (Tsuda and Katagiri 2010). As evolutionary response to effectors, many plants developed a second layer of immunity, where the recognition of effectors by specific

---

✉ Peijie Gong
gongpeijie1988@gmail.com

Michael Riemann
michael.riemann@kit.edu

Duan Dong
ddong.sh@hotmail.com

Nadja Stoeffler
nadja.stoeffler@t-online.de

Bernadette Gross
bernadettej.gross@gmail.com

Armin Markel
armin.markel@online.de

Peter Nick
peter.nick@kit.edu

[1] Botanical Institute, Karlsruhe Institute of Technology, Fritz-Haber-Weg 4, 76131 Karlsruhe, Germany

receptors can activate so-called effector-triggered immunity (ETI), which is very efficient, but usually confined to specific strains of the pathogen (Boller and He 2009; Coll et al. 2011).

While necrotrophic pathogens infect and kill host tissue to extract nutrients one time from the dead host cells, biotrophic pathogens colonise living plant tissue and obtain nutrients sustainably by reprogramming the host cell (Coll et al. 2011). The most powerful strategy against biotrophic pathogens is the HR, which is a plant-specific form of PCD. The activation of HR is often based on a long coevolution history between host plant and pathogens, associated with a high degree of plant resistance (Pontier et al. 1998). These features of HR are shared with ETI. However, the two phenomena, while often linked, can also occur independently. For instance, there are cases where ETI is not accompanied by HR (Thomma et al. 2011).

While PCD is often seen as plant version of animal apoptosis, it is not clear whether PCD and apoptosis are homologous phenomenon, because the molecular players seem to differ. Especially, the so-called caspases as central executors of apoptosis (Bröker et al. 2005) seem to be absent in higher plants. However, caspase-like regulators have been found to be essential in many cases of plant PCD (del Pozo and Lam 1998). These proteases have been reported mainly into two gene families: metacaspases and proteases with caspase-like activity (Piszczek and Gutman 2007). The latter now include VPE, proteasome, cathepsinB and phytaspase (Piszczek and Gutman 2007). The VPE are localised in the vacuoles and experiments, where they have been silenced in tobacco suggested a key role in the HR to pathogen infection (Hatsugai et al. 2004). The second family, metacasapases in sensu *strictu*, was initially linked with other forms of PCD. For instance, *McII-Pa*, a metacaspase from Norway spruce (*Picea abies*) is required to execute the PCD of the suspensor during embryogenesis (Suarez et al. 2004). However, there is also evidence for a role of metacaspases in the proper sense as regulators of HR, i.e. in a function shared with VPEs. Arabidopsis metacaspases *AtMC1* and *AtMC2* regulate HR to the obligate biotrophic oomycete *Hyaloperonospora arabidopsidis*, as well as to the hemibiotrophic bacteria *Pseudomonas syringae* pv. tomato (Coll et al. 2010).

Grapevine (*Vitis vinifera* L.) is one of the most important economical fruit species. While in Europe, only one species of the genus *Vitis* survived the Pleistocene glaciation, both North America and East Asia harbour a considerable diversity of species (Trondle et al. 2010). Especially in North America, these wild species underwent coevolution with pathogens, such as the oomycete *Plasmopara viticola*, the causative agent of downy mildew. As a result, these species might have developed a real ETI, as supported by the discovery of pathogen strains differing in host specificity (Gomez-Zeledon et al. 2013; Rouxel et al. 2013). The European wild grape (*V. vinifera* ssp. *sylvestris*) as naive host is not expected to be endowed with ETI. In fact, most cultivated varieties of *V. vinifera* ssp. *vinifera* are susceptible to downy mildew.

Introgression of genetic factors conferring pathogen resistance from American wild grapes into European varieties has been a major breakthrough in sustainable viticulture (Eibach et al. 2007). The molecular players involved in the execution of this putative HR remain to be elucidated. Metacaspase family is represented by six members in grapevine. Three members, namely *VvMC1*, *VvMC3* and *VvMC4* were found to be upregulated during ovule abortion of seedless grapes (Zhang et al. 2013), indicative of a role in developmental PCD. This leads to the central question of our current study: is there also a function of grapevine metacaspases in HR?

Our approach was to compare different grape genotypes differing with respect to the incidence of HR in response to inoculation with *P. viticola* with respect to the temporal expression of different members of VPEs and metacaspases. North American wild grape *V. rupestris* as resistant line, cv. 'Müller-Thurgau' as susceptible line was selected, and two gene candidates, namely *MC2* and *MC5* were identified as potential executors of HR. To address their cellular function, these genes were expressed as GFP fusions in tobacco BY-2 as heterologous system. Their subcellular localization was then characterised by spinning-disc confocal microscopy. Under control conditions, the expression of these grapevine metacaspases did not impair the physiology of their heterologous host. However, in response to the bacterial elicitor harpin, an inducer of PCD (Baker et al. 1993), the transgenic lines exhibited an enhanced responsiveness. By cloning different alleles of the MC2 and MC5 promoters from a *vinifera* variety not able to produce HR, and a wild grape with efficient HR, we could identify significant differences with respect to defence-related putative binding sites. However, we could also functionally confirm, using a dual-luciferase promoter-reporter assay that the metacaspase promoter alleles form the HR-competent genotype was able to drive a significantly higher expression in response to induction by the elicitor harpin. We arrive at a model where VrMC2 and VrMC5 are involved in the execution of HR, and the regulation of VrMC2 and VrMC5 expression can be linked with corresponding metacaspase promoters.

Material and methods

Plant material

Nine grapevine genotypes differing with respect to the presence of resistance loci conferring HRs: The wild North American grapevines *V. rupestris* (voucher number KIT

5888) and *V. riparia* (KIT 6548) are the presumed natural sources of the locus *Resistance to Plasmopara viticola 3* (*Rpv3*), the rootstock genotype 'Börner' (KIT 5890) derived from a cross between *V. riparia* and *V. cinerea*, and the resistant *vinifera* variety 'Regent' (KIT 5895), deriving from a complex pedigree comprising different crosses and back-crosses of different North American grapes with *vinifera* varieties and harbouring *Rpv3* (Fischer et al. 2004). In contrast, the European *vinifera* varieties 'Müller-Thurgau' (KIT 5585), 'Pinot Blanc' (KIT 7473), and 'Augster Weiss' (KIT 7443), and the European Wild Grape genotypes *V. sylvestris* 'Hö29' (KIT 6188) and *V. sylvestris* 'K83' (KIT 6235) did not experience any co-evolutionary history with this pathogen and therefore are expected to lack resistance loci, such as *Rpv3*. All genotypes are cultivated as living vouchers in the collection of the Botanical Garden of the Karlsruhe Institute of Technology, Germany and have been verified by microsatellite markers (Nick 2014). Leaf discs of 1.5 cm in diameter were collected from the fourth to the seventh leaf from the top of each shoot by means of a cork borer and used further for infection with *P. viticola*. All discs were cultivated at 22°/18 °C (day/night) and a 14 h/10 h (light/dark) photoperiod. Prior to shock freezing in liquid nitrogen for RNA extraction, a smaller (1.3-cm diameter) central disc was excised from the infected leaf disc. This 'disc-in-the-disc' harvest was employed to avoid wounding responses in the peripheral 2 mm of the disc. The frozen samples were stored at − 80 °C until extraction and analysis.

Pathogen material and inoculation

To ensure high reproducibility of results, single-sporangia strains of *P. viticola* were used. The strains 1191-B15, 1135-F2 and 1137-C20 were kindly provided by the group of Prof. Dr. Otmar Spring, Botanical Institute of Hohenheim University (Gomez-Zeledon et al. 2013). If not stated otherwise, experiments were conducted with 1191-B15, which is not able to overcome *Rpv3* mediated resistance, and induces HR on *Rpv3* positive hosts. For sporangia propagation putative regulatory elements was, the fourth to the seventh leaf of cv. 'Müller-Thurgau' shoots were detached and thoroughly rinsed at both sides with distilled water. As inoculum, mature sporangia were collected from well-infected leaves. The freshly excised leaves were placed with their abaxial side down on the surface of the sporangial suspension and kept in a phytochamber with high humidity at 21 °C in darkness for 24 h. Afterwards, leaves were turned and placed on wet filter paper with abaxial side up, incubated under a photoperiod of 16-h light (25 μmol·m^{-2}·s^{-1}) from LED-bulbs with full daylight-spectrum (TL-D Super 80 18W/840, Phillips) and 8-h darkness at 21 °C until sporulation.

To achieve controlled inoculation for the time-course experiments, the leaf discs were placed in Petri dishes on wet filter paper with their abaxial surface upwards, and a droplet of 30 μl sporangial suspension (adjusted to 40,000 sporangia ml^{-1}) was added on the centre of the abaxial surface on each disc. The Petri dishes with the infected discs were incubated at 21 °C under same conditions as given above.

Leaf disc bioassay for HR

To observe the tissue response to inoculation with strain 1191-B15, for each of the nine tested genotypes of grapevine, five leaf discs were prepared on each sampling time point (0 day, 3 days, 6 days, 9 days after *P. viticola* infection). Digital images of the infection sites were recorded using a Olympus C-5060 camera. For 'Müller-Thurgau' as representative of a *Rpv3*-negative *vinifera* cultivar, and *V. rupestris* as representative of a *Rpv3*-positive source genotype, a more detailed time course (0 h, 12 h, 24 h, 48 h, 72 h, 96 h, 120 h and 144 h after infection) was established and the presence of a potential HR was verified by digital bright-field microscopy (DM750, *Leica*, Switzerland). To detect and quantify cell death, the Evans blue dye exclusion test (Gaff and Okong'O-Ogola 1971) was used with fresh, unfixed material. Each experimental series was replicated twice in two subsequent seasons.

cDNA synthesis, semi-quantitative RT-PCR and quantitative PCR analysis of metacaspases during the local response to *P. viticola* inoculation

The frozen leaf material (from *V. rupestris*, *V. vinifera* cv. 'Müller-Thurgau') stored at − 80 °C was homogenised to a powder (Tissuelyser, Qiagen, frequency 22 Hz, duration 30 s). Then, total RNA was extracted using the Spectrum™ Plant Total RNA Kit (Sigma, Deisenhofen). The extracted RNA was purified with DNase Set (Qiagen, Hilden, Germany). First-strand cDNA synthesis was performed using M-MuLV cDNA Synthesis Kit (New England Biolabs, Germany), using 1 μg of purified RNA as template for reverse transcription. All RNA-related operations were performed on ice and in presence of a RNase inhibitor (NEB, Germany) to exclude degradation of the RNA.

Semi-quantitative RT-PCR was performed with ThermoPol buffer, dNTP and *Taq* polymerase (NEB, Germany) with 3 min of pre-denaturation at 94 °C, followed by 32 cycles of 30 s denaturation at 94 °C, 30 s annealing at 60 °C, and 40 s extension at 68 °C, conducted in a standard PCR-Thermocycler (Analytikjena, Germany) as described (Chang et al. 2011; Chang and Nick 2012; Duan et al. 2015). The accession numbers and the primer sequences are given in Supplementary Table S1 and were derived from the grapevine reference genome (*V. vinifera* cv. 'Pinot Noir'). Actin (accession number: AF369524) was used as reference gene and the amplicons were separated and evaluated by

electrophoresis on 2% agarose as described (Ismail et al. 2012). The shown images are representative for three independent experiments.

Quantitative real-time PCR was carried out on an Opticon 2 system (Bio-Rad, München) as described (Svyatyna et al. 2014) for the two promising gene candidates *VrMC2* and *VrMC5* (cloned as described below) against actin (accession number AF369524) as reference gene using a final concentrations of 200 nM for each primer, 200 nM for each dNTP, 1× GoTaq colourless buffer supplemented with 2.5 mM MgCl$_2$, 0.5 U GoTaq polymerase (Promega, Germany), 1× SYBR green I (Invitrogen, Germany), and 1 µL of the cDNA template in a 1:10 dilution (50 ng·µL^{-1}). Amplicons for the two metacaspase genes and actin were generated by denaturation at 95 °C for 3 min, followed by 40 cycles of denaturation at two steps: 95 °C for 15 s, annealing at 61 °C for 40 s. C_t values of the target gene X and those for the actin reference R were calculated as follows: The expression value on 0 h of each cultivar was set as control. Then, relative expression values were calculated as $\triangle\triangle C_t(X) = \text{Avg. } \triangle C_t(X) - \text{Avg. } \triangle C_t$ (control). The final result was expressed as $2^{-\triangle\triangle Ct}$ (X). Each result was representative for three independent experiments.

Cloning the coding sequences of *VrMC2* and *VrMC5*

Open reading frames (ORF) of *VrMC2* (1351 bp) and *VrMC5* (1245 bp) were amplified from cDNA using Phusion DNA polymerase (NEB, Germany), and the oligonucleotide primers given in Supplementary Fig. S2 derived from the grapevine genome (*V. vinifera* cv. 'Pinot Noir') via PCR by 36 cycles of 98 °C for 10 s, annealing at 58 °C for 30 s, and synthesis at 72 °C for 90 s. Following the verification of the sequence from several independent amplicons, the predicted protein sequences for *VrMC2* (accession number KY069974) and *VrMC5* (accession number KY069975) were submitted to GenBank. Afterwards, a phylogenetic tree was constructed with other 42 validated plant metacaspases, and 2 putative metacaspases from *Chlamydomonas* as algal out-group using the neighbour-joining algorithm via the MEGA 7.0 software.

Then, each of the two isolated ORFs was verified by comparison with genome (*V. vinifera* cv. Pinot Noir) and the predicted protein domains were analysed using structure tool (https://www.ncbi.nlm.nih.gov/Structure/cod/wrpsb.cgi). After alignment with ClustalW, specific primers for GATEWAY cloning were designed (Supplementary Table S2) to amplify and clone the chosen sequence into the GATEWAY® entry vector (Invitrogen Corporation, Paisley, UK). From the two entry vectors for *VrMC2* and *VrMC5*, the inserts were further ligated into the vector pH7FWG2.0 (driving expression of a fusion of the insert with a C-terminal GFP under control of the CaMV 35S promoter and a hygromycin resistance upon expression in plants) using GATEWAY LR recombination reactions. After a further verification of the

sequence, these vectors were ready for transformation of tobacco BY-2 cells.

Subcellular localization of *VrMC2* and *VrMC5* by heterologous expression in tobacco BY-2 cell culture

To address cellular aspects of metacaspase function, the tobacco BY-2 cell strain *Nicotiana tabacum* L. cv Bright Yellow 2 was used for all investigations (Nagata et al. 1992). Cells were subcultivated as described (Chang and Nick 2012). For transformation, all transgenic cell lines were generated using method (Buschmann et al. 2011) with minor modifications described in (Gao et al. 2016) mediated by chemo-competent *Agrobacterium tumefaciens* strain LBA4404 (Invitrogen Corporation, Paisley, UK).

In addition to overexpressing C-terminal GFP fusions of *VrMC2* and *VrMC5* using *pH7FWG2.0/VrMC2* and *pH7FWG2.0/VrMC5* under control of a constitutive CaMV 35S promoter (see Supplementary Fig. S5.1), one line was transformed in parallel with the empty vector *pH7FWG2.0* as negative control. Overexpressed *VrMC2* and *VrMC5* lines were done three independent times. The overexpression level of *VrMC2/5* has been checked and compared to each other (see Supplementary Fig. S8.1, S8.2). As control for a nonspecific cytosolic GFP signal, a BY-2 line expressing free GFP was kindly provided by Dr. J. Petrášek from Charles University, Prague, Czech Republic (Nocarova and Fischer 2009). Here, selective pressure was established by 25 mg L^{-1} hygromycin.

To observe and document the subcellular localization for the different transformants, GFP fluorescence was recorded via an AxioObserver Z1 (Zeiss, Jena, Germany) inverted microscope, equipped with a laser dual spinning disk scan head (Yokogawa CSU-X1 Spinning Disk Unit, Yokogawa Electric Corporation, Tokyo, Japan), a cooled digital CCD camera (AxioCam MRm; Zeiss). Images were acquired using Plan-Apochromat 63x/1.44 DIC oil objective operated via the Zen 2012 software (Blue edition). The ER was visualised by 1 µM ER-Tracker™ Red (Thermo Fisher Scientific, Germany). The GFP signal was captured using the 488-nm line, the ER-Tracker Red signal by the 561-nm line of an Ar-Kr laser.

Mortality assay in *VrMC2* and *VrMC5* overexpressing tobacco BY-2 cells in response to harpin or MeJA

To score the mortality in response to harpin (27 µg·ml^{-1}), as inducer of cell death-related immunity (Chang et al. 2011); or to MeJA (100 µM), as inducer of basal immunity, the *VrMC2*, *VrMC5* overexpressor lines were treated 1 day after subcultivation with the respective elicitor, along with the nontransformed BY-2 wild-type. Four time points 0, 24, 48 and 72 h after induction were settled. Mortality was

determined as described (Gaff and Okong'O-Ogola 1971) using the Evans Blue dye exclusion test (Fig. 6f). Afterwards, mortality value was calculated as described (Chang et al. 2011).

Cloning and analysing the promoters of *MC2* and *MC5*

Upstream promoter sequences of *MC2* and *MC5* were amplified from genomic DNA of both, *V. rupestris* and *V. vinifera* cv. 'Müller-Thurgau', using Q5® High-Fidelity DNA polymerase (NEB, Germany) based on oligonucleotide primers derived from the grapevine reference genome (*V. vinifera* cv. 'Pinot Noir') and given in Supplementary Table S2. The promoter fragments *pVvMC2* (accession number KY069976) comprising 1563 bp, and the fragment *pVvMC5*, accession number KY069978) comprising 1631 bp upstream of the start codon were both cloned from *V. vinifera* cv. 'Müller-Thurgau', whereas fragments *pVrMC2* (1554 bp, accession number KY069977), and *pVrMC5* (1599 bp, accession number KY069979) were obtained from *V. rupestris*. Amplicons were obtained using 38 cycles of 30 s annealing at 57 °C, 120 s elongation at 72 °C and 10 s denaturation at 98 °C. After elution from the gel, 0.1 μg amplicons were ligated into the pGEM®-T Easy Vector (Promega, Madison, PWl) and then transformed into *E-coli* DH5α for DNA sequencing (GATC Biotech, Cologne, Germany). The four promoter regions were further ligated into a GATEWAY version of luciferase vector pLuc (see Supplementary Fig. S5.2), kindly provided by Prof. Dr. Jochen Bogs (DLR Neustadt) using GATEWAY BP and LR recombination reactions (Invitrogen Corporation, Paisley, UK), respectively. Putative regulatory elements were analysed with the PlantCARE (http://bioinformatics.psb.ugent.be/webtools/plantcare/html/) and PLACE (http://www.dna.affrc.go.jp/PLACE/) databases (Lescot et al. 2002). Then, the two promoters were aligned by DNAMAN software and differences between the two genotypes were plotted in a map.

Assay of promoter activity by using transient transfection and a dual-luciferase reporter

To measure promoter activation, a dual-luciferase system based on transient transformation was employed (Czemmel et al. 2009) using a suspension cell line from *V. vinifera* cv. 'Pinot Noir' (Seibicke 2002) as experimental material. To calibrate the firefly luciferase luminescence against variations, the *Renilla* luciferase plasmid pRluc (see Supplementary Fig. S5.2) was transformed in parallel (Horstmann et al. 2004). For biolistic bombardment, gold particles (1.5–3.0 μM; Sigma-Aldrich, Germany) were coated with plasmid DNA, including 50 ng of specific promoter DNA and 100 ng control plasmid pRluc. Then, coated particles were loaded on macrocarriers (Bio-Rad Hercules, CA, USA) and transferred

into a custom-made chamber for shooting cells. Three-day-old cells from *V. vinifera* cv. 'Pinot Noir' placed on solid MS medium (0.8% *w/v* Danish agar) were cultivated in liquid medium as described (Chang et al. 2011) and then transiently transformed through three shots at a pressure of 1.5 bar in a vacuum chamber of − 0.8 bar, as described (Duan et al. 2016).

Promoter activation was measured in response to elicitation by either 27 μg·ml^{-1} harpin, 100 μM MeJA, or without elicitation 24 h after bombardment. Cells were harvested using a Büchner funnel and homogenised in 150 μl of 2× passive lysis buffer (PLB, Promega, Madison, WI) by grinding on ice with a pestle in a mortar for 1.5 min. Luciferase and *Renilla* enzyme-substrate activity were measured using a commercial dual-luciferase reporter substrate (PJK, Kleinblittersdorf, Germany), and luminescence was measured through a Lumat LB9507 luminometer (Berthold Technologies, Bad Wildbad, Germany). All experiments were repeated in three independent series. Mean values of the ratios between firefly and *Renilla* luciferase luminescence were recorded as readout of luciferase activity normalised for transformation efficiency and relative changes of activity calculated over the values measured in the nontreated samples. Vectors *pSTS29/pLuc* and *MYB14/pART7* (Holl et al. 2013) were used as positive controls and kindly provided by Prof. Dr. Jochen Bogs (DLR Neustadt).

Results

Plant metacaspases diversity in different clades in different taxa

Previously, we had identified and characterised in silico the entire grape metacaspase family from the reference genome of *V. vinifera* cv. 'Pinot Noir' by a BLAST search based on the available sequences of *A. thaliana* metacaspase proteins (Zhang et al. 2013). To get further insight into the evolutionary history and phylogenetic relationships of the plant metacaspases, a neighbour-joining tree was constructed based on the protein sequence alignment of 42 *bona-fide* metacaspases from higher plants and two putative metacaspases from the alga *Chlamydomonas* (Fig. 1). From the constructed tree, two major clusters (clades 1 and 2) emerged. Clade 1 comprised 20 type-I metacaspases and was further divided into three subclades (I–III), while clade 2 comprised 22 type-II metacaspases and also was divided into three subclades (IV–VI). The separation between subclade I versus subclades II/III was supported by a high bootstrap value (above 90%), whereas the separation between subclades II and III was not so significant (bootstrap values around 70%).

Based on specific features of their regulation (see below), two metacaspase homologues named *VrMC2*
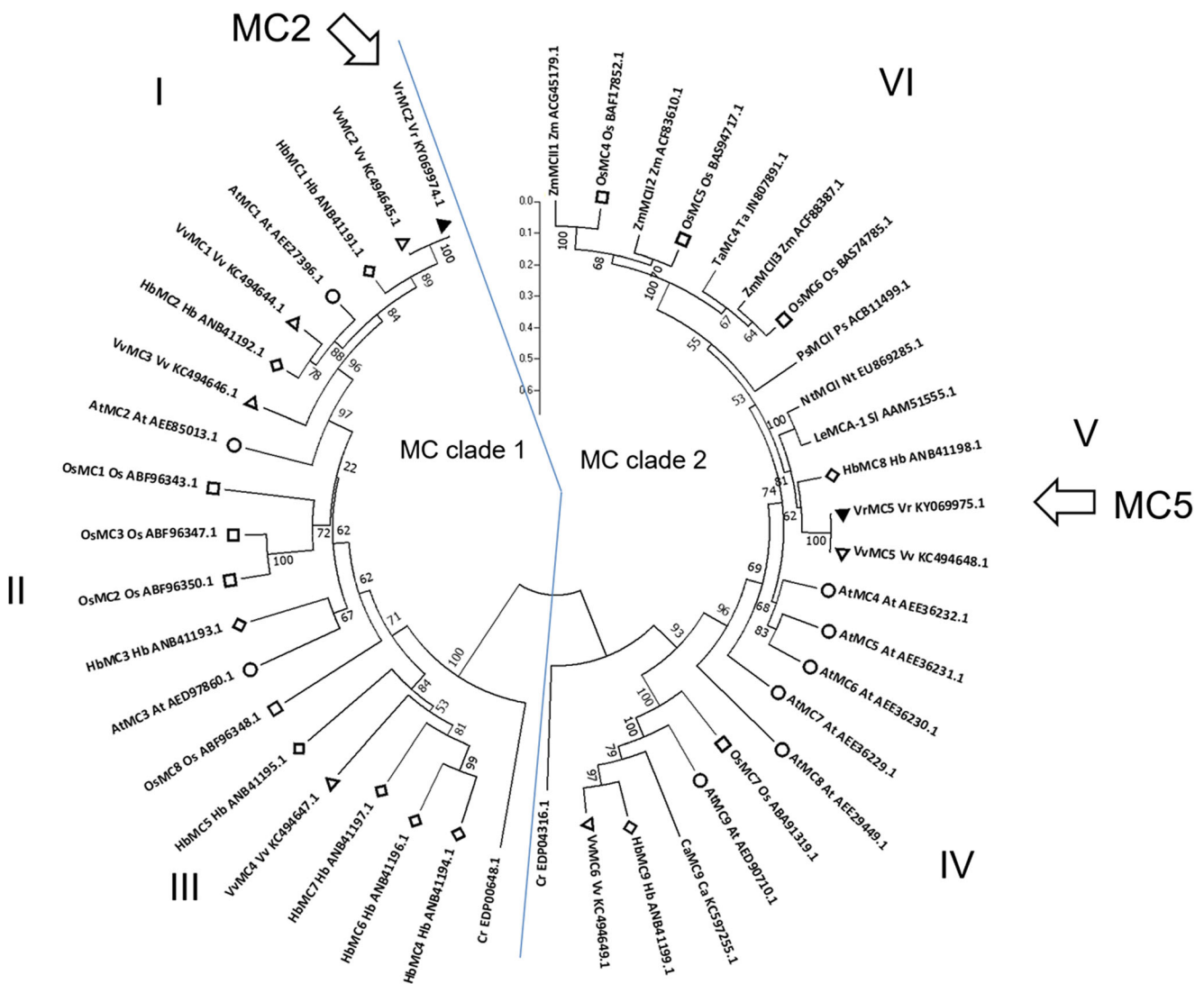
Fig. 1 Molecular phylogeny constructed by the neighbour-joining algorithm on well-known 42 metacaspase genes. The position of the VrMC2 and VrMC5 sequence from *V. rupestris* is indicated by two arrows. Values next to the branches represent the percentage of replicate trees in which the associated taxa clustered together in the bootstrap test (based on 500 replicates). Green circles (○) indicated whole metacaspase family of *Arabidopsis*. Pink frame (□) indicated whole metacaspase family of *Oryza sativa*. Hollow yellow triangle (△) indicated whole metacaspase family of *Vitis vinifera*. Full-filled yellow triangle (▲) indicated metacaspase2 and metacaspase5 of *V. rupestris*. Hollow brown rhombus (◇) indicated whole metacaspase family of *Hevea brasiliensis*. Unmarked branches are incomplete metacaspase family members from *Zea mays* L. (maize), *Triticum aestivum* (wheat), *Capsicum annuum* L. (pepper), *Lycopersicon esculentum* Mill. (tomato), *Nicotiana tabacum* (tobacoo), *Picea abies* (Norway spruce), separately. The acronym of metacaspase genes were named using the first letter of the genus followed by the first letter of the species, plus related Swiss-Prot accession numbers

(GenBank accession no. KY069974 (Fig. 1), and *VrMC5* (GenBank accession no. KY069975, Fig. 1) were successfully cloned from the *V. rupestris*. Not surprisingly, these two sequences were almost identical to their already identified homologues from *V. vinifera* cv. 'Pinot Noir' (only 2–4 amino acid exchanges in the variable regions, Supplementary Fig. S1). Besides, two metacaspases predicted from *Chlamydomonas* genome were found basal at the two clades, indicating that these clades are evolutionary ancient and might reflect different functions of the metacaspase family (Fig. 1).

Resistance to *P. viticola* in *V. rupestris* correlates with HR-like necrosis

We investigated possible differences in the incidence of HR along with differences in susceptibility to *P. viticola*. Our approach was to inoculated a panel of nine grape genotypes with the single-sporangium strain 1191-B15. The panel comprised the *Rpv3* positive resistant vinifera variety 'Regent' along with *V. rupestris* and *V. riparia* as potential source of *Rpv3*, three *Rpv3* negative susceptible *vinifera* varieties, and three *sylvestris* genotypes that due to their European origin were

expected to lack *Rpv3*. We followed the local responses over time after controlled infection of leaf discs, starting from inoculation at day 0 over 6 and 9 days post infection (dpi) until inspection of sporulation at 9 dpi (Fig. 2). Necrotic spots indicative of HR became visible even to the naked eye from 3 dpi in *V. riparia*, *V. rupestris*, and also from 6 dpi in *V. vinifera cv.* 'Regent'. Interestingly, the *V. sylvestris* genotype Hoe29 also showed very few spots, but only after 9 dpi. In contrast, even at 9 dpi no necrotic spots were observed on the susceptible *V. vinifera* cultivars 'Augster Weiss', 'Müller-Thurgau' or 'Pinot Blanc'. Furthermore, the appearance of necrotic spots in *V. riparia*, *V. rupestris* and *V. vinifera cv.* 'Regent' correlated with a reduction of pathogen sporulation (Fig. 2). In contrast, the *vinifera* cultivars which were not displaying HR-like lesions, where seen to carry sporulations from 6 dpi. Three genotypes displayed different amplitudes of a third pattern: the *sylvestris* genotypes 'Hö29' and (much less pronounced) 'Ke83' supported only a reduced level of sporulation, but rarely produce necrotic lesions. The extreme of this third pattern was seen in the rootstock genotype 'Börner' (deriving from a cross between *V. riparia* and *V. cinerea*), where neither necrotic lesions nor sporulations were apparent.

Based on this screening experiment, *V. vinifera cv.* 'Müller-Thurgau' as susceptible, and *V. rupestris* as resistant genotype were selected for a more detailed analysis (Fig. 3a). Every single necrotic spot developed around a stoma in the centre surrounded by an expanding area of dead cells was observed

and verified by Evans Blue staining (Fig. 3b). Cell death could be observed from 48 hpi and frequency of the necrotic spots increased with the time after inoculation. To further quantify this phenomenon, infection sites were scanned by reflection bright-field microscopy and the diameters of the lesions were quantified (Supplementary Fig. S2). This quantification revealed that necrotic lesions became detectable from 24 hpi, and first increased in number reaching a plateau from 72 hpi, while spot size rapidly increased after 96 hpi, followed by a slower expansion of necrosis. These results were also corroborated by the intensity of the Evans blue staining, which steadily intensified with time after inoculation (Supplementary Fig. S3). In contrast, no lesions appeared on *V. vinifera cv.* 'Müller-Thurgau' nor water controls. Instead, when the concentration of sporangia was progressively increasing in cv. 'Müller-Thurgau' from 4 dpi, that had reached a level that was approximately 30-fold as compared to that seen in *V. rupestris* at 10 dpi (Supplementary Fig. S2).

Expression of *VrMC2* and *VrMC5* respond to infection by *P. viticola* and correlates with cell death

We have shown previously that specific members of the grapevine metacaspase gene family are upregulated during the key stage of ovule abortion in seedless grapes (Zhang et al. 2013). We also wanted to find out whether the HR response to the biotrophic pathogen *P. viticola* might be
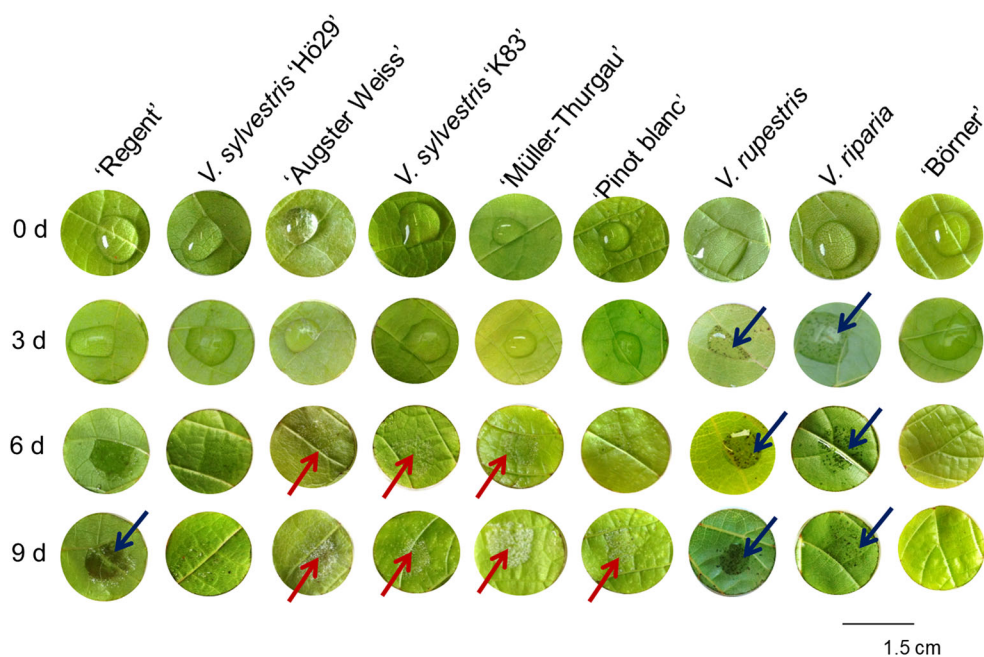
Fig. 2 Leaf disc phenotype of nine different grapevine varieties at four time points after *Plasmopara viticola* 1191-B15 infection. Pictures were taken at 0, 3, 6, 9 d (days) after infection. From left to right: *V. vinifera* Regent, *V. vinifera* ssp. *sylvestris* Hoe29, *V. vinifera* Augster Weiss, *V. vinifera* ssp. *sylvestris* K 83, *V. vinifera cv.* Mueller Thurgau,

V. vinifera cv. Pinot blanc, *V. rupestris*, *V. riparia* and *V. boerner* (*V. riparia × V. cinerea*). A droplet of 30 μl sporangial suspension (adjusted to 40,000 sporangia. ml⁻¹) was added on the centre of the abaxial surface on each leaf disc. Blue arrows, necrotic spots; orange arrows, sporulation; bar = 1.5 cm
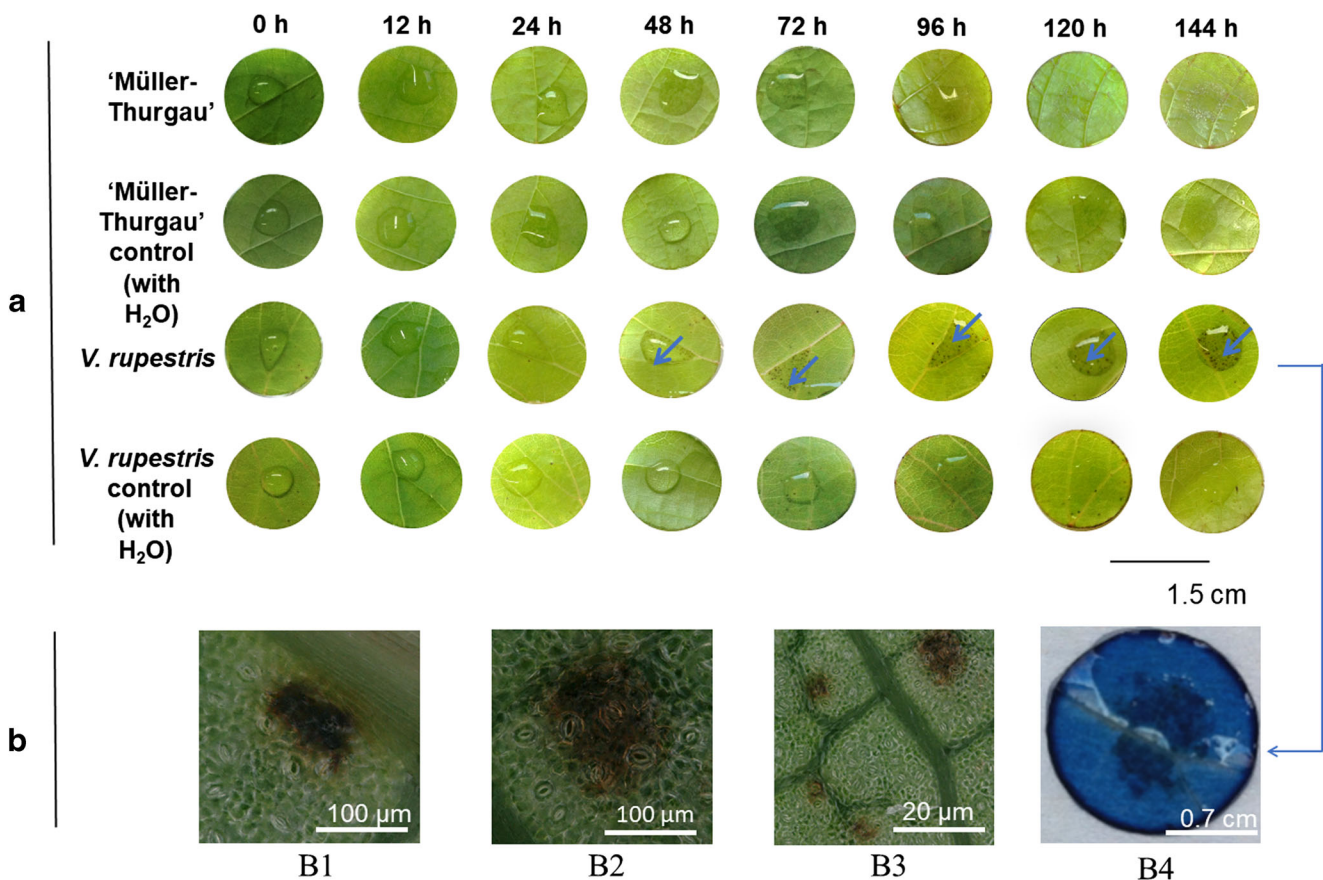
Fig. 3 Necrotic spots in leaf discs of *V. vinifera* cv. Mueller Thurgau and *V. rupestris* at eight time points after *Plasmopara viticola* 1191-B15 infection. **a**. Pictures were taken at 0 h, 12 h, 24 h, 48 h, 72 h, 96 h, 120 h and 144 h after *P. viticola* infection. Blue arrows indicate necrotic spots. These regions of local cell death could be observed only in *V. rupestris* from 48 h post-infection (hpi). Distilled H₂O-treated samples are shown as negative control in parallel. **b**. Micrographs and staining after infection on *V. rupestris*. B1, necrotic spots under 20× magnification at 48 hpi; B2, necrotic spots under 20× magnification at 144 hpi; B3, necrotic spots under 10× magnification at 144 hpi; B4, cell death appeared in areas showing a dark-blue staining by 2.5% (*w/v*) Evans blue

associated with specific members of the metacaspase family? Towards that goal we analysed the pathogen response of steady-state transcript levels for metacaspase genes under the same set-up as in Fig. 2 as above.

While *MC4* and *MC6* were not expressed in leaf discs at all, *MC3* expressed also weakly (Supplementary Fig. S4.1). *MC1* was upregulated in both host genotypes, but only at late time points after HR occurrence (Fig. 4a). In contrast, *VrMC2* and *VrMC5* transcripts were specifically upregulated at 24 hpi (Fig. 4a). This was neither seen in infected *V. vinifera* cv. 'Müller-Thurgau' as a host, nor was it found in mock-inoculated leaf discs from *V. rupestris*. The patterns of *VrMC2* and *VrMC5* in *V. rupestris* were then verified by quantitative PCR (Fig. 4b). While transcript levels were not induced in the mock control with expression values fluctuating between 0.5–1.5, both *VrMC2* and *VrMC5* increased transiently to more than twofold of the starting level at 24 hpi, and then dropped back at 48 hpi to the control level.

In addition, to further validate our results, we tested two additional single-sporangia strains of *P. viticola*: strain 1135-F2 was comparable to 1191-B15 with respect to infection behaviour, whereas strain 1137-C20 was able to break *Rpv3*-mediated resistance of the *vinifera* cultivar 'Regent' (Gomez-Zeledon et al. 2013). We conducted a time-course experiment and analysed *MC2* and *MC5* at 0 hpi, 24 hpi, 48 hpi and 96 hpi by semi-quantitative RT-PCR on *V. vinifera* cv. 'Müller-Thurgau' and *V. rupestris* (Supplementary Fig. S4.2). Again, *VrMC2* and *VrMC5* on the *V. rupestris* host increased transiently at 24 hpi for both pathogen strains, whereas on *V. vinifera* cv. 'Müller-Thurgau', there was no obvious upregulation.

Based on these expression patterns, these two genes, *VrMC2 and VrMC5*, were prioritised as central candidates to clarify their subcellular localization, cellular function and the regulatory features of their promoters.

VrMC2 and VrMC5 exhibit differential subcellular localization

To get insight into potentially different functions of VrMC2 (belonging to clade 1) and VrMC5 (belonging to clade 2),

'Müller Thurgau' treated by control (with dH$_2$O)

'Müller Thurgau' infected by B15

V. rupestris treated by control (with dH$_2$O)

V. rupestris infected by B15
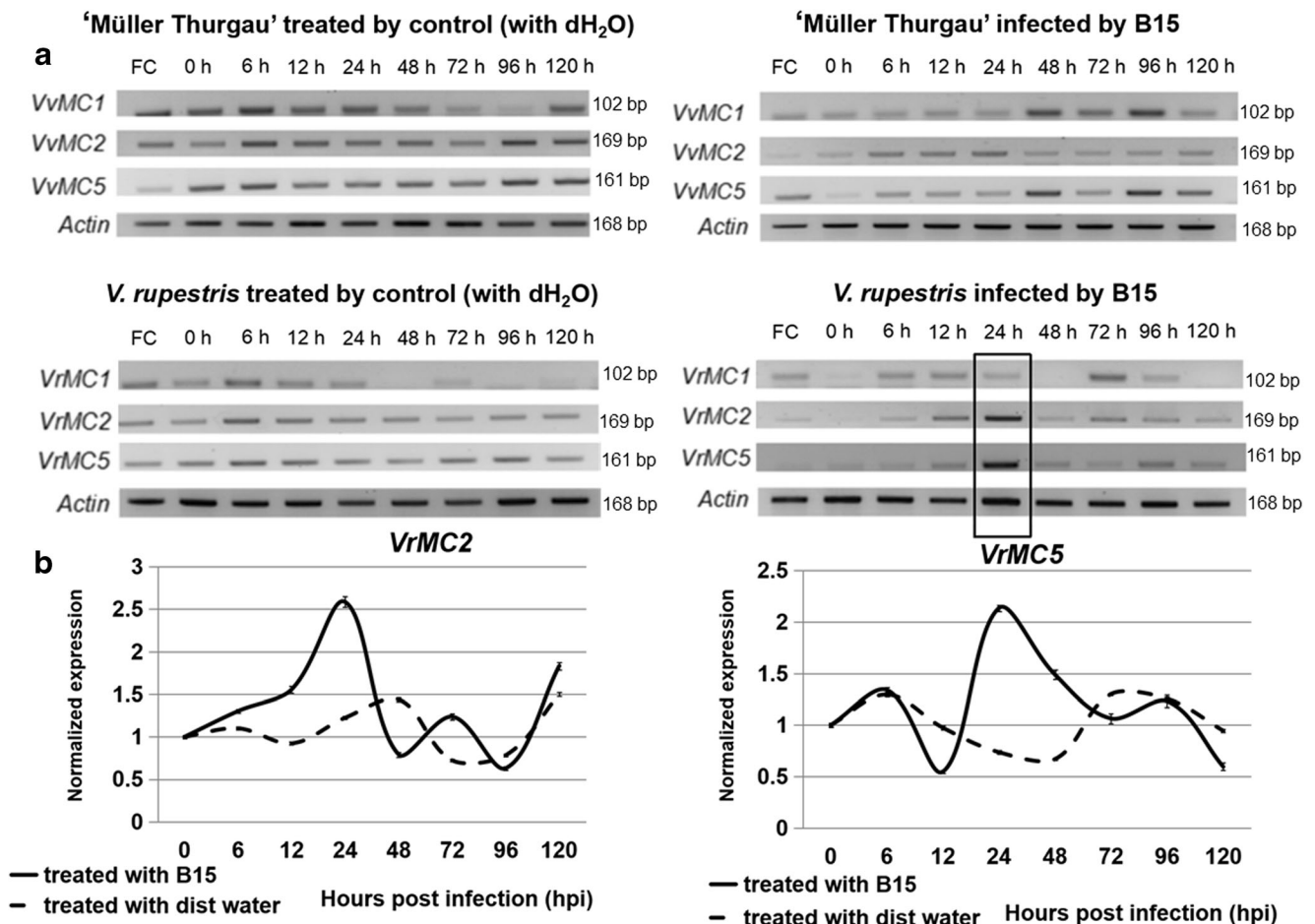
Fig. 4 Gene expression analysis of grape *MC1*, *MC2* and *MC5* genes during *P. viticola* 1191-B15 infection. **a** Representative agarose gels with the amplified transcripts of MC1, MC2 and MC5 on *V. vinifera* cv. 'Mueller Thurgau' and *V. rupestris* by semi-quantitative RT-PCR. FC (as fresh control), 0 h, 6 h 12 h, 24 h, 48 h, 72 h, 96 h and 120 h (corresponding time points with Fig. 3) were set as time points after inoculation with 1191-B15. Actin was tested and compared as internal reference gene. Distilled H$_2$O-treated samples were used as negative control in parallel. Representative images from three independent experimental series are shown. **b** Quantitative PCR expression assays of *VrMC2* and *VrMC5* genes induced by 1191-B15 infection on *V. rupestris*. Quantification of transcripts of metacaspase 2 (*VrMC2*) and metacaspase 5 (*VrMC5*) at 0 h, 6 h 12 h, 24 h, 48 h, 72 h, 96 h and 120 h (consistent time points with Fig. 3) after inoculation by quantitative real-time PCR. Actin was tested as internal reference gene. The result of a representative experiment is shown. Standard errors were calculated by three technical replicates. Data represent mean from three independent experimental series

subcellular localization was addressed after *Agrobacterium*-mediated transformation of *VrMC2/MC5* fused with GFP into tobacco BY-2 cells using spinning-disc confocal microscopy (Fig. 5). As negative control, an empty vector only harbouring only the 35S promoter was transfected in parallel. In this case, no fluorescent signal was detected (Fig. 5a). A line expressing free GFP cell line was used as positive control. The GFP signal was distributed across cytoplasm and nucleus (Fig. 5b). The results showed that VrMC2-GFP was located exclusively around the nuclear zone. A faint fluorescent signal was scattered around the plasma membrane (Fig. 5c).

The localization in cytoplasmic strands and the reticulate-vesicular appearance of the signal indicated that the fusion protein was localised in the ER. To further test this hypothesis, the specific dye ER-Tracker Red was used for dual visualisation of ER along with the GFP signal indicative of VrMC2.

Results showed VrMC2 GFP signals were inlaid in the form of positioning on the RFP fluorescence of ER. (Supplementary Fig. S6.1). In contrast, *35S*::VrMC5-GFP was distributed homogeneously in cytoplasm and even in the nucleus (Fig. 5d, details in Supplementary Fig. S6.2), thus resembling the pattern seen for free GFP. The differences in subcellular localization suggested that the two different types of grape metacaspases may differ with respect to their function.

Harpin can induce HR on overexpressed cell lines of *VrMC2* and *VrMC5*

To get insight into a potential function of *VrMC2* and *VrMC5* as executors of PCD, the BY-2 lines, transformed with *35S*::*VrMC2-GFP* and *35S*::*VrMC5-GFP*, were exposed to
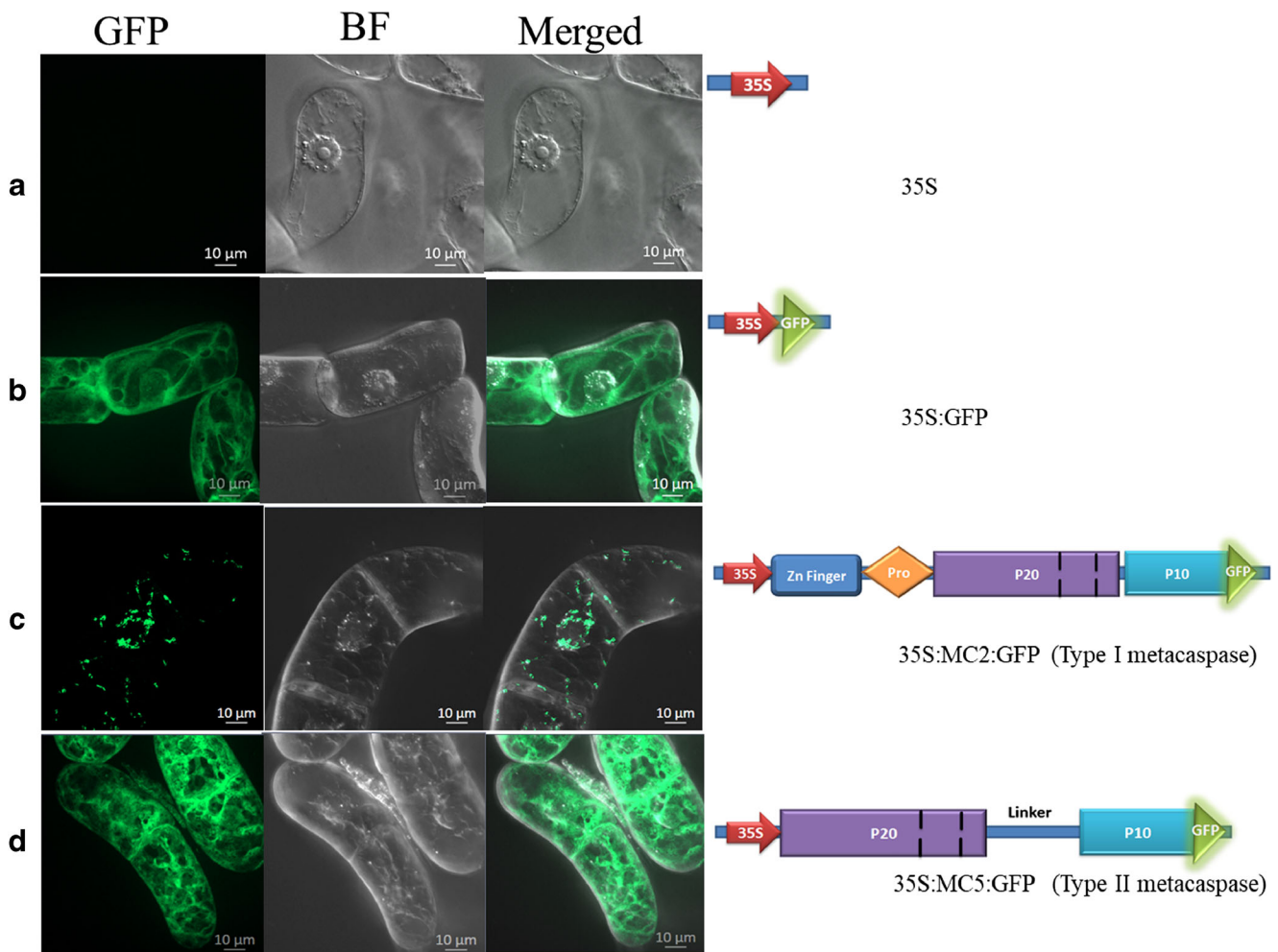
Fig. 5 Subcellular localization of OxVrMC2-GFP (C-terminal) and OxVrMC5-GFP (C-terminal) transient transformation in BY-2 suspension cells. Left to right: GFP, the channel of green fluorescence signal; BF, bright field; merged, combine channel of GFP and BF. **a** Empty vector (35S:) as negative control; **b** enhanced green fluorescence signal of free GFP (35S:GFP) as positive control; **c** VrMC2 localization (35S:VrMC2:GFP); **d** VrMC5 localization (35S:VrMC5:GFP); all transgenic cell lines were generated via agro-bacteria transformation. VrMC2 and VrMC5 fused with GFP tag was overexpressed into BY2 tobacco cells using *pH7FWG2.0* vector. GFP fluorescence was recorded via an AxioObserver Z1 (Zeiss, Germany) inverted microscope, equipped with a laser dual spinning disk scan head. Scale bar represents 10 μm. All representative images are shown as the confocal sections from a *z*-stack along with a differential-interference contrast (DIC) image

harpin, a bacterial elicitor that can trigger PCD in plant cells (Chang and Nick 2012), and the resulting mortality was evaluated during 3 days. As reference, a nontransformed BY-2 line (WT) was included. All three lines were first followed over time in the absence of elicitor (Fig. 6a). In this control experiment, mortality was maintained at a very low and stable level of around 2.5%. Likewise, addition of exogenous MeJA (100 μM), while inducing a slight, but significant increase in mortality (up to 5–7%), did not release any difference between the nontransformed line and the two lines expressing the foreign metacaspase fusions.

Our previous studies had shown that harpin-induced HR cell death in suspension cells of *Vitis* (Chang and Nick 2012). We therefore tested the response of the three cell lines to 27 μg·ml^{-1} harpin to detect a potential activity of the expressed fusion protein in the execution of cell

death (Fig. 6c). In fact, already at 24 h after treatment, mortality had increased significantly (to 9.7%) in the nontransformed WT, while the mortality in both, the VrMC2-GFP and the VrMC5-GFP, cell lines had risen even higher (14.6 and 17%, respectively). For the subsequent time points, the differences were even amplified: While mortality in the WT was remaining at 10%, it increased in both transgenic lines (more slowly in the VrMC5-GFP expressor, in a more pronounced manner in the VrMC2-GFP expressor) and had reached 26.6% (VrMC5-GFP line), and even 33.3% in the VrMC2-GFP line. To test potential synergies between MeJA and harpin, we used 100 μM MeJA treatment in combination with the harpin treatment. Instead of a synergy, we observed an antagonistic effect: for both transgenic lines, MeJA clearly mitigated the activation of cell death by
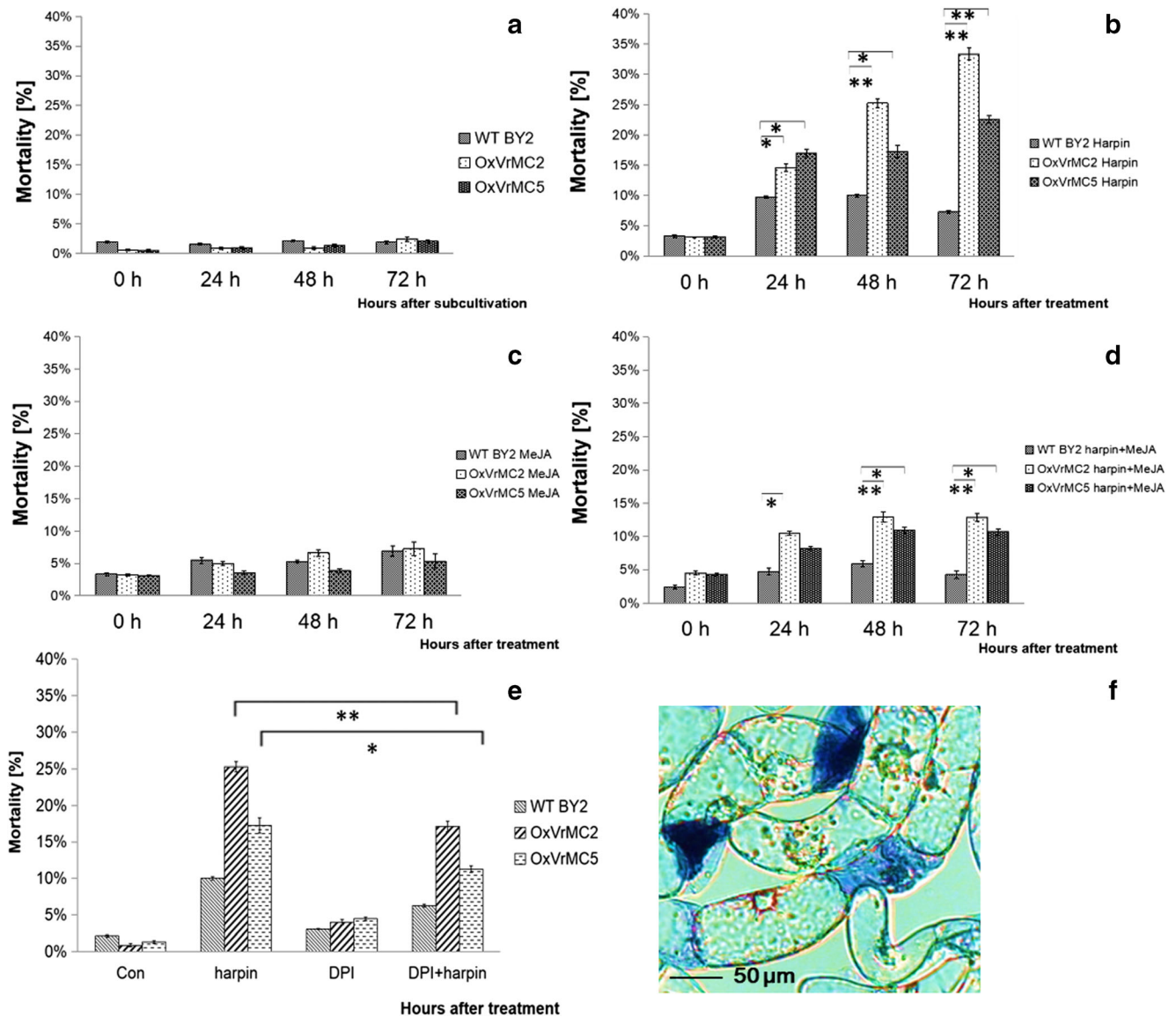
Fig. 6 Cell mortality assays of suspension cell lines after harpin, harpin+ DPI and MeJA elicitation. Wild-type and transformed cells were cultivated at 26 °C in 100-ml Erlenmeyer flasks on an orbital shaker at 150 rpm. Every 7 days by inoculation of 6 or 8 ml of stationary cells into 30 ml of fresh, autoclaved liquid MS medium (Murashige and Skoog). The columns show the relative frequency of dead cells of Ox-*VrMC2* and Ox-*VrMC5* as compared to wild-type BY2 control under normal condition **a** under normal cultivation, control, **b** after 27 μg·ml^{-1} harpin treatment, **c** after 100 μM MeJA (methyl jasmonate) treatment, **d** after 100 μM MeJA + 27 μg·ml^{-1} harpin treatment. **e** Effect of the NADPH oxidase inhibitor

diphenyleneiodonium (DPI) on cell death of VrMC2 and VrMC5 overexpressors induced by harpin. Mortality was scored after 48 h of treatment with DPI (0.2 μM), harpin (27 μg·ml^{-1}1), or the combination of both in non-transformed BY-2 versus Ox-*VrMC2* and Ox-*VrMC5*. A single asterisk indicates differences that are statistically significant on the $P < 0.05$ level. Double asterisks indicate differences that are statistically extreme significant on the $P < 0.01$ level. Mean values and standard errors from three independent experimental series are shown. **f** A representative figure of Ox-*VrMC2* suspension cells staining by 2.5% (*w/v*) Evans blue after 24 h of 27 μg·ml^{-1} harpin treatment

27 μg·ml^{-1} harpin (compare Fig. 6b, d). Even in the nontransformed WT, MeJA reduced mortality to a degree that the induction by harpin was completely prevented.

These results imply that expression of *VrMC2-GFP* and *VrMC5-GFP* confer an elevated responsiveness to harpin as elicitor able to trigger a HR-like response in cell culture. This

elevated responsiveness can be eliminated, when harpin is administered in presence of MeJA. This not only tells that MeJA and harpin act antagonistically, but it also tells that the transgenic lines do not show elevated mortality per se, but only in response to a trigger that can induce cell death (this conclusion is also supported by the finding that the

transgenic lines are perfectly viable in the absence of harpin, and even in their response to MeJA alone (Fig. 6a, c).

Apoplastic oxidative burst by ROS participates in the mechanism responsible for the VrMC2 and VrMC5-dependent cell death

A rapid oxidative burst triggered by a plasma membrane-located NADPH oxidase, is correlated with activation of cell death by harpin treatment in *V. rupestris* suspension cells (Chang and Nick 2012). Specific NADPH oxidase inhibitor DPI was used here to quell this oxidative burst before elicitating cell death by harpin, to test whether this oxidative burst is necessary for VrMC2/VrMC5-mediated cell death. In fact, DPI significantly suppressed harpin-induced mortality in all three cell lines (Fig. 6e), while DPI alone did not affect viability in a significant manner. The mitigation of cell death was most pronounced for the VrMC2-GFP line. These data indicated that the plasma membrane-located NADPH oxidase participates in the mechanism responsible for the VrMC2/VrMC5-dependence of harpin-triggered cell death.

Cis-element comparison of the promoters *pMC2* and *pMC5* between *V. vinifera* cv. 'Müller-Thurgau' and *V. rupestris*

To get insight into the regulatory features of the two prime metacaspase candidates, we cloned for all four promoter regions (*pMC2* and *pMC5* from both *V. vinifera* cv. 'Müller-Thurgau and *V. rupestris*) 1500~1600 bp upstream of the translational start codon. The alignment of these putative promoter regions revealed a high degree of identity (around 95%) between the *pMC2* from *V. vinifera* cv. 'Müller-Thurgau' (abbreviated as *pVvMC2*, GenBank: KY069976), and *V. rupestris* (abbreviated as *pVrMC2*, GenBank: KY069977), as well as between the *pMC5* from *V. vinifera* cv. 'Müller-Thurgau'

(abbreviated as *pVvMC5*, GenBank: KY069978) and *V. rupestris* KY069979).

Putative cis-elements were predicted from the *V. rupestris* as compared to their *vinifera* counterparts (see, Table 1). The two *pMC2* regions harbour significantly more defence cis-elements as compared to the respective *pMC5* regions (Fig. 7a). In the case of *pMC2*, the allele of *V. rupestris* harbours two GT-1 motives, predicted to be involved in the response to pathogen and salt stress, as well as one as-1/ocs-like element motif involved in spectral defence (Chen et al. 2002; Park et al. 2004). These three predicted motives are not found in the *pMC2* allele from cv. 'Müller-Thurgau'. Likewise, the *pMC5* allele from *V. rupestris* contains three predicted BIHD1OS motives, proposed as regulator of disease resistance (Luo et al. 2005). Again, this element is absent the *pMC5* allele from *V. vinifera* cv. 'Müller- Thurgau'. It should be mentioned that none of the four putative promoter alleles contained any of the known jasmonate-related response elements or enhancers (detail see, Table 2).

Harpin activates promoter activity of both *pVrMC2* and *pVrMC5*

To test, whether activation of cell death-related defence by harpin is accompanied by activation of promoter activity, the dual-luciferase reporter assay system (Holl et al. 2013) was employed in a suspension culture of *V. vinifera* cv. 'Pinot Noir', which, by itself, shows only a low cell death activity (Chang and Nick 2012). We used co-expression of a stilbene-synthase promoter, *pSTS29/pLuc*, and its transcriptional activator, *MYB14/pART7*, as a positive control to verify the stability of the system (Holl et al. 2013). Compared to expression of *pSTS29/pLuc* alone, the co-expression with this transcriptional activator stimulated luciferase activity by a factor of 8 (Supplementary Fig. S7), which is consistent with published results (Holl et al. 2013).

Table 1 Cis-element distribution analysis of PMC2 and PMC5 promoters related on pathogen or stress defence response

Name	Sequence	Numbers		Function	Reference
		*pMC2*MT-Rup	*pMC5*MT-Rup		
GT-1 motif	GAAAAA	4–6	4–3	Pathogen and salt stress	Rao et al. (2010)
W-box	TGAC	5–5	3–5	Wound and defence response	Eulgem et al. (2000)
W-box	TGACT	1–0	1–0	Wound and defence response	Maleck et al. (2000)
W-box	TTGAC	3–4	0–0	Stress response to environmental influences	Chen et al. (2002)
W-box	TTGACC	1–1	0–0	Fungal elicitor responsive element	Kumar et al. (2009)
as-1/ocs element-like	TGACG	0–1	1–1	Pathogen response	Chen et al. (2002)
BIHD1OS	TGTCA	0–1	0–3	Disease resistance response	Luo et al. (2005)
TC-rich repeats	ATTTCTTCA	0–0	1–0	Defence and stress responsiveness	Diaz-De-Leon et al. (1993)
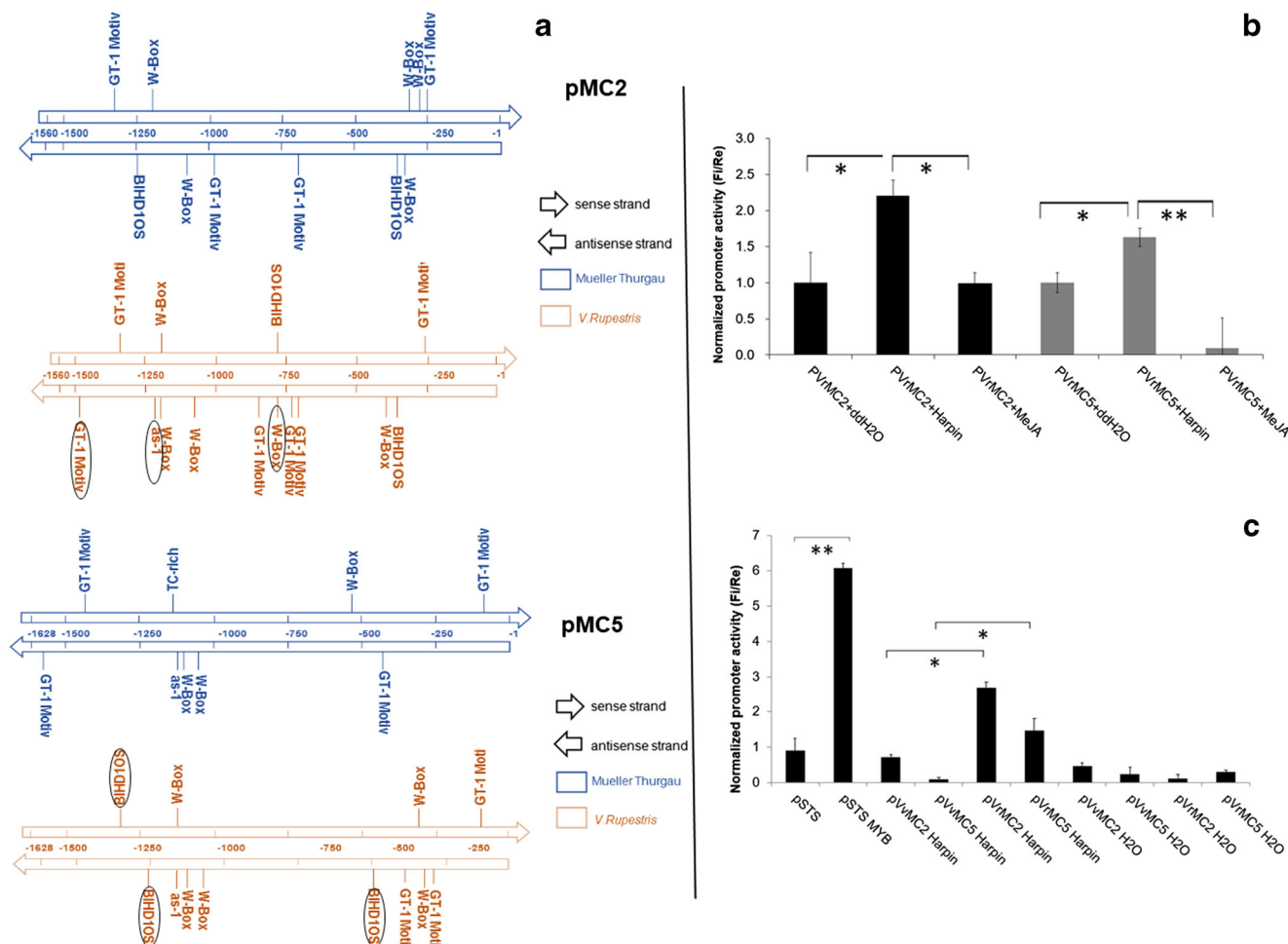
Fig. 7 Cis-element distribution analysis and dual-luciferase assay for comparison of pMC2, pMC5 promoter activity between *V. vinifera* cv. 'Mueller Thurgau' and *V. rupestris*. **a** Cis-element distribution in both upstream and downstream sequences of the MC2, MC5 promoter of *V. vinifera* cv. Mueller Thurgau (black) and *V. rupestris* (grey), all pathogen response-related elements were showed. The number scale refers to the base pairs before the initiation codon ATG of the respective gene. **b** Dual-luciferase test of pMC2, pMC5 promoter activity in *V. rupestris* after harpin and MeJA treatment. **c** Dual-luciferase test of pMC2, pMC5 promoter activity between *V. vinifera* cv. 'Mueller Thurgau' and *V. rupestris* after harpin and MeJA treatment. All plasmids were transfer to *V. v* cv. 'Pinot Noir' cells transiently using gene gun bombardment technique. Y-axis value is promoter activity, which equal to firefly luciferase activity value divided Renilla luciferase activity. The columns show the relative activity values of *pVrMC2*, *pVrMC5*, *pVvMC2* and *pVvMC5* promoters with sterile-distilled H_2O as negative control and normalised induction level at 24 h after 27 μg/ml harpin. A single asterisk indicates differences that are statistically significant on the $P < 0.05$ level. Double asterisks indicate differences that are statistically extreme significant on the $P < 0.01$ level

In the second step, we measured the activation of the *VrMC2* and *VrMC5* promoters in response to the elicitor harpin (27 μg·ml^{-1}) compared to a mock treatment with sterilised water as a solvent control, which did not produce any significant modulation of promoter activity, neither for *pVrMC2* nor for *pVrMC5* (Fig. 7b). By contrast, the activity of *pVrMC2* in response to harpin was induced by 120% and the activity of *pVrMC5* by 60%. Since the analysis of putative cis-elements had not uncovered any of the known jasmonate-response elements, we also measured promoter activations in response to 100 μM MeJA. Neither the activity of *pVrMC2* nor that of *pVrMC5* was activated by MeJA. Surprisingly, the activity of pVrMC5 was even completely repressed by MeJA. We further measured the harpin response of the respective promoter alleles from *V. vinifera* cv. 'Müller-Thurgau'. No activity stimulation was found on *pVvMC2* and *pVvMC5* (Fig. 7c). The results further confirmed that *pVrMC2* was more responsive to harpin elicitation than *pVrMC5*.

Overall, the pattern seen in the promoter activity assay for induction with the elicitor harpin was consistent with that found for gene expression in leaf discs upon a compatible interaction with the pathogen *P. viticola* (Fig. 4): In both cases, the induction was around twofold. Interestingly, in contrast to harpin, MeJA was not able to activate the metacaspase promoters.

Table 2 Cis-element distribution analysis of PMC2 and PMC5 promoters related on hormone response

Name	Sequence	Amount in		Function	Reference
		MC2MT-Rup	MC5MT-Rup		
ASF1MOTIFCAMV	TGACG	0–1	1–1	Gene activation by auxin and SA	Despres (2003)
ELRECOREPCRP1	TTGACC	1–1	0–0	Activation of PR- and WRKY-genes	Laloi et al. (2004)
GT1CONSENSUS	GRWAAW	16–15	8–7	SA-inducible gene expression	Zhou (1999)
MARABOX1	AATAAAYAAA	4–4	0–0	A-box in SAR	Gasser et al. (1989)
MARARS	WTTTATRTTTW	1–1	0–0	Found in SAR	Gasser et al. (1989)
MARTBOX	TTWTWTTWTT	8–5	1–0	T-box; found in SAR	Gasser et al. (1989)
WBOXATNPR1	TTGAC	2–3	0–0	Part of SA-answer	Xu et al. (2006)

Discussion

In our previous work (Zhang et al. 2013), we have described the entire gene family of grapevine metacaspases on the sequence level. We also provided evidence for a role of certain metacaspase members in a developmental event of PCD (ovule abortion in seedless grapes). Since the HR differs qualitatively from developmental PCD (Lam 2004), we asked the question, whether a different set of metacaspase members might be involved here. In fact, when we followed temporal patterns of expression during compatible versus incompatible interaction of different grapevine genotypes with *P. viticola*, we identified *MC2* and *MC5* as candidates for a function in HR. We found MC2 located at the ER, while MC5 was nucleocytoplasmic. Overexpression in tobacco cells enhanced PCD in response to the bacterial elicitor harpin. This effect was mitigated by inhibition of NADPH oxidases, or by supplementing with methyl jasmonate, a crucial signal of basal immunity. Both findings are consistent with a role of MC2 and MC5 in cell death-related immunity. The promoter alleles of the two genes isolated from *V. rupestris*, a grape with very efficient HR, harbour numerous motives predicted to be linked with defence. Using a dual-luciferase reporter system in grapevine cells, we show that these alleles are also more responsive to harpin consistent with the regulatory pattern observed in infected leaf discs, while they were not induced (or even repressed) by MeJA as signal linked with basal immunity. These findings support a model, where MC2 and MC5 act specifically as executors of the HR.

Different tools to kill yourself? Functional specificities of metacaspases

A phylogenetic reconstruction of available metacaspase sequences over the different divisions of land plants shows that metacaspases are always represented in two clades, which can be seen already in the model *Chlorophyte Chlamydomonas*. This indicates some functional specialisation. Interestingly, also the two metacaspases linked with the HR of grapevine represent both clades—MC2 is part of clade 1, while MC5 represents clade 2. It is conceivable that the two metacaspases convey different and possibly complementary functions in defence-related cell death. To conclude that complementary action of two metacaspase types is a condition sine qua non for PCD would not be appropriate; however, the developmentally induced PCD executing ovule abortion has been shown to involve *VvMC1*, *VvMC3* and *VvMC4* (Zhang et al. 2013), and these three metacaspases are all members of clade 1. Thus, already from the conservation of the two metacaspase clades, and from the differential regulation of metacaspase members, it is evident that the members of this gene family are not functionally redundant, but convey specific functions linked with the specific differences of the respective type of PCD (for instance, developmental cell death versus HR).

A similar induction of transcripts has also been reported in the context of other HRs. For instance, the type-II metacaspase TaMCA4 from wheat is upregulated during the compatible interaction with *Puccinia striiformis* f. sp. *tritici* (Wang et al. 2012). Transient overexpression of this metacaspase promoted resistance stimulated the resulting HR, while interference with its expression impaired both, resistance and development of a necrotic reaction.

Functional specificity of the different metacaspases is also supported by the observation of tissue-specific expression: While *VvMC4* was specifically expressed in the stem, *VvMC6* was dominantly active in flowers (Zhang et al. 2013), and *βVPE* and *δVPE* were expressed specifically in ovules. Our results demonstrate that these genes are silent in leaves and not inducible by *P. viticola*. Two further members, *MC1* and *MC3*, were expressed in leaves, but their transcript levels were not related with a HR and might rather be linked with other forms of cell death, for instance, a wounding response triggered by the excision of the leaf discs. In addition, under the three know VPE members, only *VrγVPE* was specifically upregulated by infection in *V. rupestris* from 24 hpi. By

using genotype (being incompetent or competent for a HR) and dependence on the pathogen (mock control versus sporangia) as logical filters, exclusively the expression of *VrMC2* and *VrMC5* matched the criteria, and therefore seem to be specific for the HR.

This evidence for functional specificity of different metacaspase members is congruent with reports from Arabidopsis, where AtMC8 was required for UVC stress-induced cell death (He et al. 2008), while AtMC4 mediates PCD activation by the fungal toxin FB1 and abiotic stress inducers (Suarez et al. 2004). And in Norway spruce (*Picea abies*), McII-Pa is required for embryogenesis-associated PCD (He et al. 2008; Suarez et al. 2004; Watanabe and Lam 2011). Thus, there seem to be different metacaspases used as tools to execute different types of PCD.

VrMC2 and VrMC5 exhibit differential subcellular localization

While MC5 was nucleocytoplasmic and lacked any canonical organelle-targeting signal, as had been reported for the rice homologues OsMC5 and OsMC6 (Huang et al. 2015) and AtMC4 (Watanabe and Lam 2011), MC2 was seen to be localised in the ER consistent with the presence of a C-terminal predicted retention-like motif (KPFI). In addition, an N-terminal zinc-finger domain was predicted by the PSORT algorithm (http://psort.ims.u-tokyo.ac.jp/) in Supplementary Table S3. However, no canonical nuclear-localization sequence was detected (reported for some type-I metacaspases). The same zinc-finger motif mediates interaction with LSD proteins, negative regulators of PCD, in case of AtMC1 (Coll et al. 2010). This ER-localization contrasts with that of the MC2 homologue from rice, OsMC1, which was reported to be exclusively localised in the nucleus probably because it contains an NLS in the N-terminal region (Huang et al. 2015). From our results, MC2 GFP co-colalisation showed highlight spots, it might trigger an interesting question: if MC2 is localised on Golgi also?

Thus, the clade-I member MC2 shows the by far more specific localization pattern and, also amplifies the death response to harpin more efficiently than MC5. It would therefore by rewarding to test the possibility, whether it can modulate subcellular localization in response to signals as had been reported for Arabidopsis AtMC9 that can aggregate during late autolysis (Bollhoner et al. 2013). From Fig. S6.2, it seems MC5 showed a bit of a mesh sub-loc just adjacent to the nucleus. We inferred that MC5 might overlapped with ER to some extent. We also observed that MC5 is similar with location of GFP free cell, but it still has some unique features. Therefore, more specific localisation pattern of MC5 is needed to further research.

What did we learn about early signals?

To dissect signals that are activating metacaspase activity, we used the approach to overexpress *MC2* and *MC5* under control of the CaMV-35S promoter in tobacco BY-2 cells. While these cells were perfectly viable under control conditions, we were able to amplify the cell death response to harpin (most pronounced for MC2). Since the 35S-promoter drives constitutive expression, transcriptional activation does not play a role here. Therefore, the observed amplification must depend exclusively on posttranscriptional regulation (such as proteolytic activation of silent pro-metacaspase proteins). The signalling of the ETI-like response to harpin has been mapped for grapevine suspension cells and compared to the signalling deployed by the PAMP flg22 (Chang and Nick 2012). In both cases, an apoplastic oxidative burst (caused by activation of the NADPH oxidase RboH) and an influx of calcium are crucial. The temporal sequence, however, is inverted: in basal immunity, the calcium influx is first, the oxidative burst follows later, in the ETI-like immunity, calcium influx is late and preceded by a more rapid oxidative burst. A second crucial difference is the efficient accumulation of jasmonic acid and its active isoleucine conjugate in response to flg22, a phenomenon that does not occur during the ETI-like response to harpin (Chang et al. 2017). In the current work, we can show that diphenylene iodonium, a specific inhibitor of NADPH oxidases, can partially quell the amplification of the harpin response in the metacaspase overexpressors. Thus, superoxide generated during this early signalling event is important to activate metacaspase activity.

A similar partial suppression is achieved by exogenous methyl jasmonate. Accumulation of jasmonic acid has been reported for defence-related cell death in *vitis* leaves leading to the idea that jasmonic acid might be an activator of PCD (Repka et al. 2004). On the other hand, jasmonic acid negatively regulates cell death in *A. thaliana* under oxidative stress caused by ozone treatment. Conversely, the mycotoxin fumonisin B1 (FB1) can initiate PCD in *Arabidopsis* by disrupting a part of jasmonate signalling through activation of antagonistic salicylic-acid pathway (Zhang et al. 2015). Our observations from the current study clearly support jasmonic acid as negative regulator of metacaspase mediated cell death.

These findings can be integrated in the following working model (Fig. 8): Pathogen effectors are thought to be recognised by nucleotide-binding leucine-rich repeat (NB-LRR) receptors NB-LRRs in plants which often, but not always, results in a HR (Coll et al. 2011; Takken and Tameling 2009). We used the bacterial elicitor harpin to elicit an ETI-like response in cell culture. Whether harpin is binding to a NB-LRR receptor, is not clear. The affinity of harpin for its binding site is in the range of μM range, which speaks against a role of NB-LRR receptors in harpin-triggered signalling.
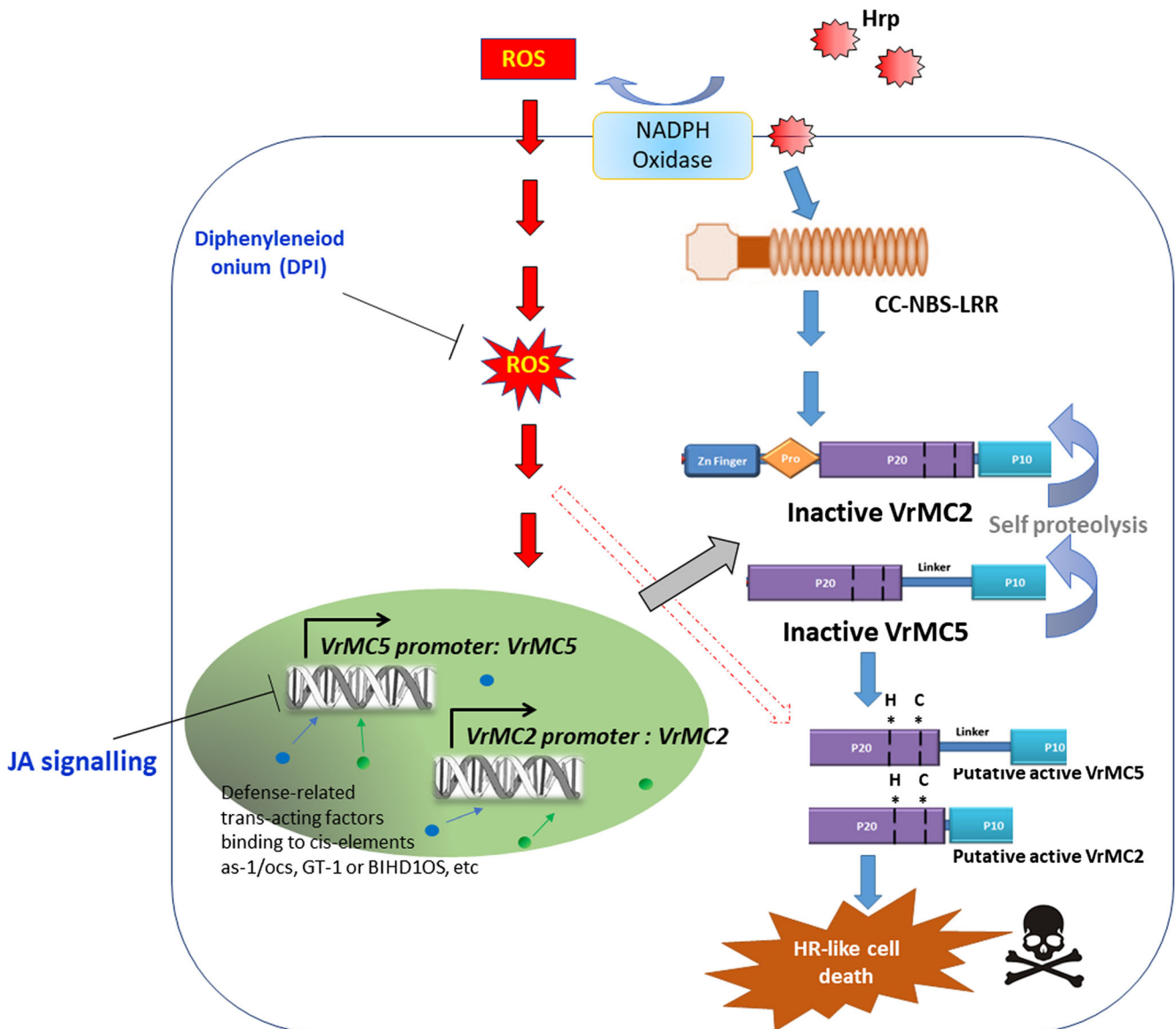
Fig. 8 Model for VrMC2- and VrMC5-mediated HR-like cell death-related signalling induced by harpin as effector-like elicitor. The diagram represents some of the characteristic features of VrMC2 and VrMC5-mediated HR-like cell death that could occur in response to HR elicitor stimulation in plants. Details are explained in the text. Hrp, harpin as bacteria elicitor; CC-NBS-LRR, N-terminal-coiled coil domain, nucleotide-binding site, leucine-rich repeats, as R receptors to recognise elicitor; NADPH, nicotinamide adenine dinucleotide phosphate hydrogen; ROS, reactive oxygen species; JA/MeJA, jasmonic acid/methyljasmonate; HR, hypersensitive response

However, in both cases, a stimulation of the membrane-bound NADPH oxidase RboH is causing an increased production of apoplastic ROS that could enter the cytoplasm, for instance through aquaporin channels (Chaumont and Tyerman 2014). This rapid increase of ROS in the absence of jasmonic acid would, in the first stage, activate metacaspase activity on the posttranscriptional level. In case of basal immunity, where jasmonate signalling is deployed (Chang et al. 2017), the ROS activation of metacaspase activity is suppressed. Moreover, in case of basal immunity, the activation of RboH would be a later event that is preceded by calcium influx, a

MAP-kinase cascade and activation of phytoalexin genes as well as of jasmonate signalling genes. These rapid metacaspase responses are later supported or sustained, in a second stage, by a transcriptional activation of *VrMC2* and *VrMC5* promoters. Again, RboH is necessary and jasmonate signalling acts negatively. Whether these signals act through a signal chain that differs from posttranslational activation, remains to be elucidated. An alternative model might be that the consumption of metacaspase pro-proteins by their proteolytic activation is sensed and triggers a replenishing transcriptional response.

Outlook

The two-stage model of metacaspase activation developed in this work shifts the focus on the signals that act upstream of proteolytic cleavage. Apoplastic oxidative burst has been shown to be necessary for this activation, but is it sufficient? Why is the (late) apoplastic burst in basal immunity not activating cell death—is it just a matter of timing or the accumulation of inhibitory jasmonate? Is the proteolytic activation of metacaspases sufficient to trigger metacaspase promoter activation, or are additional signals required? To provide answers to these questions, we are currently developing strategies to interfere with metacaspase activity on the level of enzyme activity to test, how this will feed back on transcriptional activation. A second research question is linked with the specific localization pattern seen for MC2—is it possible to identify signals that make this protein repartition into the nucleus or interact with regulatory binding proteins such as grapevine homologues of AtLSD1? Given the fact that metacaspases can exert proteolytic functions in addition to execute PCD (Klemencic and Funk 2018), there must be additional regulatory levels to ensure that activation of the pro-protein can be stopped from deploying the entire cell death programme. In order to achieve these future research projects, it is needed to obtain stable plants of MC2 and MC5 in grape varieties. These regulation levels are probably to be searched at the posttranslational level and could involve protein modification, or dynamic relocation.

According to our work model, we summarised the signal transmission pathway of HR after the pathogen effector invasion. Especially, we identified key factors which induce HR in relative downstream, for the ultimate implementation of HR. Since we only see the function of cell death in the MCA gene in *V. rupestris*, we advocate the use of North American grape disease resistance traits as a resource to improve the status of *V. vinifera* susceptible pathogen disease.

Compliance with ethical standards

References

Baker CJ, Orlandi EW, Mock NM (1993) Harpin, an elicitor of the hypersensitive response in tobacco caused by *Erwinia amylovora*, elicits active oxygen production in suspension cells. Plant Physiol 102:1341–1344

Boller T, He SY (2009) Innate immunity in plants: an arms race between pattern recognition receptors in plants and effectors in microbial pathogens. Science 324:742–744. https://doi.org/10.1126/science.1171647

Bollhoner B, Zhang B, Stael S, Denance N, Overmyer K, Goffner D, Van Breusegem F, Tuominen H (2013) Post mortem function of AtMC9 in xylem vessel elements. New Phytol 200:498–510. https://doi.org/10.1111/nph.12387

Bröker LE, Kruyt FAE, Giaccone G (2005) Cell death independent of caspases: a review clinical. Cancer Res 11:3155–3162. https://doi.org/10.1158/1078-0432.ccr-04-2223

Buschmann H, Green P, Sambade A, Doonan JH, Lloyd CW (2011) Cytoskeletal dynamics in interphase, mitosis and cytokinesis analysed through Agrobacterium-mediated transient transformation of tobacco BY-2 cells. New Phytol 190:258–267. https://doi.org/10.1111/j.1469-8137.2010.03587.x

Chang XL, Nick P (2012) Defence signalling triggered by flg22 and harpin is integrated into a different stilbene output in *vitis* cells. PLoS One 7(7):e40446. https://doi.org/10.1371/journal.pone.0040446

Chang X, Heene E, Qiao F, Nick P (2011) The phytoalexin resveratrol regulates the initiation of hypersensitive cell death in *Vitis* cell. PLoS One 6(10):e26405. https://doi.org/10.1371/journal.pone.0026405

Chang XL, Seo M, Takebayashi Y, Kamiya Y, Riemann M, Nick P (2017) Jasmonates are induced by the PAMP flg22 but not the cell death-inducing elicitor harpin in *Vitis rupestris*. Protoplasma 254:271–283. https://doi.org/10.1007/s00709-016-0941-7

Chaumont F, Tyerman SD (2014) Aquaporins: highly regulated channels controlling plant water relations. Plant Physiol 164:1600–1618. https://doi.org/10.1104/pp.113.233791

Chen WQ, Provart NJ, Glazebrook J, Katagiri F, Chang HS, Eulgem T, Mauch F, Luan S, Zou GZ, Whitham SA, Budworth PR, Tao Y, Xie ZY, Chen X, Lam S, Kreps JA, Harper JF, Si-Ammour A, Mauch-Mani B, Heinlein M, Kobayashi K, Hohn T, Dangl JL, Wang X, Zhu T (2002) Expression profile matrix of *Arabidopsis* transcription factor genes suggests their putative functions in response to environmental stresses. Plant Cell 14:559–574. https://doi.org/10.1105/tpc.010410

Coll NS, Vercammen D, Smidler A, Clover C, Van Breusegem F, Dangl JL, Epple P (2010) Arabidopsis type I metacaspases control cell death. Science 330:1393–1397. https://doi.org/10.1126/science.1194980

Coll NS, Epple P, Dangl JL (2011) Programmed cell death in the plant immune system. Cell Death Differ 18:1247–1256. https://doi.org/10.1038/cdd.2011.37

Czemmel S, Stracke R, Weisshaar B, Cordon N, Harris NN, Walker AR, Robinson SP, Bogs J (2009) The grapevine R2R3-MYB transcription factor VvMYBF1 regulates flavonol synthesis in developing grape berries. Plant Physiol 151:1513–1530. https://doi.org/10.1104/pp.109.142059

del Pozo O, Lam E (1998) Caspases and programmed cell death in the hypersensitive response of plants to pathogens. Curr Biol 8:1129–1132. https://doi.org/10.1016/s0960-9822(98)70469-5

Despres C (2003) The Arabidopsis NPR1 Disease Resistance Protein Is a Novel Cofactor That Confers Redox Regulation of DNA Binding Activity to the Basic Domain/Leucine Zipper Transcription Factor TGA1. Plant Cell Online 15(9):2181–2191

Diaz-De-Leon F, Klotz KL, Lagrimini LM (1993) Nucleotide-Sequence of the Tobacco (Nicotiana-Tabacum) Anionic Peroxidase Gene. Plant Physiol 101:1117–1118. https://doi.org/10.1104/pp.101.3.1117

Duan D, Halter D, Baltenweck R, Tisch C, Tröster V, Kortekamp A, Hugueney P, Nick P (2015) Genetic diversity of stilbene metabolism in *Vitis sylvestris*. J Exp Bot 66:3243–3257. https://doi.org/10.1093/jxb/erv137

Duan D, Fischer S, Merz P, Bogs J, Riemann M, Nick P (2016) An ancestral allele of grapevine transcription factor MYB14 promotes

plant defence. J Exp Bot 67:1795–1804. https://doi.org/10.1093/jxb/erv569

Eibach R, Zyprian E, Welter L, Töpfer R (2007) The use of molecular markers for pyramiding resistance genes in grapevine breeding. Vitis 46:120–124

Eulgem T, Rushton PJ, Robatzek S, Somssich IE (2000) The WRKY superfamily of plant transcription factors Trends. Plant Sci 5:199–206. https://doi.org/10.1016/S1360-1385(00)01600-9

Fischer BM, Salakhutdinov I, Akkurt M, Eibach R, Edwards KJ, Topfer R, Zyprian EM (2004) Quantitative trait locus analysis of fungal disease resistance factors on a molecular map of grapevine TAG theoretical and applied genetics. Theoretische und angewandte Genetik 108:501–515. https://doi.org/10.1007/s00122-003-1445-3

Gaff DF, Okong'O-Ogola O (1971) The use of non-permeating pigments for testing the survival of cells. J Exp Bot 22:756–758. https://doi.org/10.1093/jxb/22.3.756

Gao N, Wadhwani P, Muhlhauser P, Liu Q, Riemann M, Ulrich AS, Nick P (2016) An antifungal protein from Ginkgo biloba binds actin and can trigger cell death. Protoplasma 253:1159–1174. https://doi.org/10.1007/s00709-015-0876-4

Gomez-Zeledon J, Zipper R, Spring O (2013) Assessment of phenotypic diversity of Plasmopara viticola on Vitis genotypes with different resistance. Crop Prot 54:221–228. https://doi.org/10.1016/j.cropro.2013.08.015

Gasser SM, Amati BB, Cardenas ME, Hofmann JF (1989) Studies on scaffold attachment sites and their relation to genome function. Int Rev Cytol 119:57–96

Hatsugai N, Kuroyanagi M, Yamada K, Meshi T, Tsuda S, Kondo M, Nishimura M, Hara-Nishimura I (2004) A plant vacuolar protease, VPE, mediates virus-induced hypersensitive cell death. Science 305:855–858. https://doi.org/10.1126/science.1099859

He R, Drury GE, Rotari VI, Gordon A, Willer M, Farzaneh T, Woltering EJ, Galloi P (2008) Metacaspase-8 modulates programmed cell death induced by ultraviolet light and H2O2 in Arabidopsis. J Biol Chem 283:774–783. https://doi.org/10.1074/jbc.M704185200

Holl J, Vannozzi A, Czemmel S, D'Onofrio C, Walker AR, Rausch T, Lucchin M, Boss PK, Dry IB, Bogs J (2013) The R2R3-MYB transcription factors MYB14 and MYB15 regulate stilbene biosynthesis in Vitis vinifera. Plant Cell 25:4135–4149. https://doi.org/10.1105/tpc.113.117127

Horstmann V, Huether CM, Jost W, Reski R, Decker EL (2004) Quantitative promoter analysis in Physcomitrella patens: a set of plant vectors activating gene expression within three orders of magnitude. BMC Biotechnol 4:13. https://doi.org/10.1186/1472-6750-4-13

Huang L, Zhang H, Hong Y, Liu S, Li D, Song F (2015) Stress-responsive expression, subcellular localization and protein-protein interactions of the rice metacaspase family. Int J Mol Sci 16:16216–16241. https://doi.org/10.3390/ijms160716216

Ismail A, Riemann M, Nick P (2012) The jasmonate pathway mediates salt tolerance in grapevines. J Exp Bot 63:2127–2139. https://doi.org/10.1093/jxb/err426

Jones JD, Dangl JL (2006) The plant immune system. Nature 444:323–329. https://doi.org/10.1038/nature05286

Klemencic M, Funk C (2018) Structural and functional diversity of caspase homologues in non-metazoan organisms. Protoplasma 255:387–397. https://doi.org/10.1007/s00709-017-1145-5

Kumar GM, Mamidala P, Podile AR (2009) Regulation of Polygalacturonase-inhibitory proteins in plants is highly dependent on stress and light responsive elements. Plant Omics 2:238–249

Laloi C (2004) The Arabidopsis Cytosolic Thioredoxin h5 Gene Induction by Oxidative Stress and Its W-Box-Mediated Response to Pathogen Elicitor. Plant Physiol 134(3):1006–1016

Lam E (2004) Controlled cell death, plant survival and development. Nat Rev Mol Cell Biol 5:305–315. https://doi.org/10.1038/nrm1358

Lescot M, Dehais P, Thijs G, Marchal K, Moreau Y, Peer Y, Rouze P, Rombauts S (2002) PlantCARE, a database of plant cis-acting regulatory elements and a portal to tools for in silico analysis of promoter sequences. Nucleic Acids Res 30:325–327

Luo H, Song F, Goodman RM, Zheng Z (2005) Up-regulation of OsBIHD1, a rice gene encoding BELL homeo-domain transcriptional factor, in disease resistance responses. Plant Biol 7:459–468. https://doi.org/10.1055/s-2005-865851

Maleck K, Levine A, Eulgem T, Morgan A, Schmid J, Lawton KA, Dangl JL, Dietrich RA (2000) The transcriptome of Arabidopsis thaliana during systemic acquired resistance. Nat Genet 26(4):403–410

Nagata T, Nemoto Y, Hasezawa S (1992) Tobacco BY-2 Cell Line as the "HeLa" Cell in the Cell Biology of Higher Plants. Int Rev Cytol 132:1–30. https://doi.org/10.1016/S0074-7696(08)62452-3

Nick P (2014) Schützen und nützen - von der Erhaltung zur Anwendung. Fallbeispiel Europäische Wildrebe. Handbuch Genbank WEL Hoppea Denkschr Regensb Bot Ges Sonderband:159–173

Nocarova E, Fischer L (2009) Cloning of transgenic tobacco BY-2 cells; an efficient method to analyse and reduce high natural heterogeneity of transgene expression. BMC Plant Biol 9:44. https://doi.org/10.1186/1471-2229-9-44

Park HC, Kim ML, Kang YH, Jeon JM, Yoo JH, Kim MC, Park CY, Jeong JC, Moon BC, Lee JH, Yoon HW, Lee SH, Chung WS, Lim CO, Lee SY, Hong JC, Cho MJ (2004) Pathogen- and NaCl-induced expression of the SCaM-4 promoter is mediated in part by a GT-1 box that interacts with a GT-1-like transcription factor. Plant Physiol 135:2150–2161. https://doi.org/10.1104/pp.104.041442

Piszczek E, Gutman W (2007) Caspase-like proteases and their role in programmed cell death in plants. Acta Physiol Plant 29:391–398. https://doi.org/10.1007/s11738-007-0086-6

Pontier D, Balague C, Roby D (1998) The hypersensitive response. A programmed cell death associated with plant resistance. Cr Acad Sci Iii-Vie 321:721–734. https://doi.org/10.1016/S0764-4469(98)80013-9

Rao S, El-Habbak M, Haudenshield JS, Zheng D, Hartman GL, Korban SS, Ghabrial SA (2010) Over-expression of the calmodulin gene SCaM-4 in soybean enhances resistance to Phytophthora sojae. Phytopathology 100:S107–S107

Repka V, Fischerova I, Silharova K (2004) Methyl jasmonate is a potent elicitor of multiple defense responses in grapevine leaves and cell-suspension cultures. Biol Plant 48:273–283. https://doi.org/10.1023/B:BIOP.0000033456.27521.e5

Rouxel M, Mestre P, Comont G, Lehman BL, Schilder A, Delmotte F (2013) Phylogenetic and experimental evidence for host-specialized cryptic species in a biotrophic oomycete. New Phytol 197:251–263. https://doi.org/10.1111/nph.12016

Seibicke T (2002) Untersuchungen zur induzierten Resistenz a Vitis spec. PhD thesis University of Freiburg

Suarez MF, Filonova LH, Smertenko A, Savenkov EI, Clapham DH, von Arnold S, Zhivotovsky B, Bozhkov PV (2004) Metacaspase-dependent is essential for PCD in plant embryogenesis. Curr Biol 14:339–340. https://doi.org/10.1016/j.cub.2004.04.019

Svyatyna K, Jikumaru Y, Brendel R, Reichelt M, Mithofer A, Takano M, Kamiya Y, Nick P, Riemann M (2014) Light induces jasmonate-isoleucine conjugation via OsJAR1-dependent and -independent pathways in rice. Plant Cell Environ 37:827–839. https://doi.org/10.1111/pce.12201

Takken FLW, Tameling WIL (2009) To nibble at plant resistance proteins. Science 324:744–746. https://doi.org/10.1126/science.1171666

Thomma BP, Nurnberger T, Joosten MH (2011) Of PAMPs and effectors: the blurred PTI-ETI dichotomy. Plant Cell 23:4–15. https://doi.org/10.1105/tpc.110.082602

Trondle D, Schroder S, Kassemeyer HH, Kiefer C, Koch MA, Nick P (2010) Molecular phylogeny of the genus Vitis (Vitaceae) based on plastid markers. Am J Bot 97:1168–1178. https://doi.org/10.3732/ajb.0900218

Tsuda K, Katagiri F (2010) Comparing signaling mechanisms engaged in pattern-triggered and effector-triggered immunity. Curr Opin Plant Biol 13:459–465. https://doi.org/10.1016/j.pbi.2010.04.006

Wang X, Feng H, Tang C, Bai P, Wei G, Huang L, Kang Z (2012) TaMCA4, a novel wheat metacaspase gene functions in programmed cell death induced by the fungal pathogen *Puccinia striiformis* f. sp. *tritici*. Molecular plant-microbe interactions. MPMI 25:755–764. https://doi.org/10.1094/MPMI-11-11-0283-R

Watanabe N, Lam E (2011) Arabidopsis metacaspase 2d is a positive mediator of cell death induced during biotic and abiotic stresses. Plant J 66:969–982. https://doi.org/10.1111/j.1365-313X.2011.04554.x

Xu SX, Liu GS, Chen RD (2006) Characterization of an anther- and tapetum-specific gene and its highly specific promoter isolated from tomato. Plant Cell Rep 25(3):231–240

Zhang CH, Gong PJ, Wei R, Li SX, Zhang XT, Yu YH, Wang YJ (2013) The metacaspase gene family of *Vitis vinifera L.*: characterization and differential expression during ovule abortion in stenospermocarpic seedless grapes. Gene 528:267–276. https://doi.org/10.1016/j.gene.2013.06.062

Zhang X, Wu Q, Cui S, Ren J, Qian W, Yang Y, He S, Chu J, Sun X, Yan C, Yu X, An C (2015) Hijacking of the jasmonate pathway by the mycotoxin fumonisin B1 (FB1) to initiate programmed cell death in *Arabidopsis* is modulated by RGLG3 and RGLG4. J Exp Bot 66:2709–2721. https://doi.org/10.1093/jxb/erv068

Zhou DX (1999) Regulatory mechanism of plant gene transcription by GT-elements and GT-factors. Trends Plant Sci 4:210–214